

# The Reggeized model for $\gamma p \rightarrow \rho^- \Delta^{++}(1232)$ photoproduction

Byung-Geel Yu\* and Kook-Jin Kong†

Research Institute of Basic Sciences, Korea Aerospace University, Goyang, 412-791, Korea

(Dated: December 8, 2016)

We construct a model for the reaction process  $\gamma p \rightarrow \rho^- \Delta^{++}$  by utilizing the Reggeization of the  $t$ -channel meson exchange and present the analysis of the existing data at high energies. Based on the simple  $\pi + \rho$  exchanges where the  $t$ -channel  $\rho$  exchange is conserved with the  $u$ -channel  $\Delta$ -pole in addition to the  $s$ -channel proton pole and the contact term, we discuss the convergence of the reaction cross section at high energy in association with the gauge prescription for the  $u$ -channel  $\Delta$ -pole as well as the proton-pole in the  $s$ -channel. The roles of the electromagnetic (EM) multipole moments of the  $\Delta$ -baryon and  $\rho$ -meson are analyzed. The agreement of the present calculation with the data of total and differential cross sections and spin density matrix elements for the  $\gamma p \rightarrow \rho^- \Delta^{++}$  process are shown. Model predictions for the measurements of the electromagnetic moments of the  $\rho$  and  $\Delta$  are given to the photon polarization asymmetry.

PACS numbers: 11.55.Jy, 13.60.Rj, 13.60.Le, 13.85.Fb, 14.20.Gk, 14.40.Be

Keywords:  $\Delta(1232)$  and  $\rho$  photoproduction, Gauge invariance Electromagnetic multipole moments, Regge trajectory

Photoproduction of charged  $\rho$  with  $\Delta$ -baryon in the final state is one of the issues which have been less challenged despite its significance to our understanding of the interaction between hadrons of higher spins.

To date, however, few theoretical investigations are found in literature to treat hadron productions of such high-spins by electromagnetic probe, though the energy, angle and polarization dependences of the reaction cross sections had been measured for the reaction  $\gamma p \rightarrow \rho^- \Delta^{++}$  in various photon energies more than forty years ago [1][2][3–6].

With empirical evidences of  $\rho\Delta$  formation in the final state from the analysis of the reaction process  $\gamma p \rightarrow p\pi^+\pi^0\pi^-$ , a theoretical study of the  $\gamma p \rightarrow \rho^- \Delta^{++}$  process was attempted in Ref. [7], but limited only to a construction of the Born approximation amplitude with a special gauge prescription applied for the  $\rho$  exchange. The analysis of the  $\gamma p \rightarrow \rho^- \Delta^{++}$  process by using the  $\pi + b_1 + \rho + a_2$  Regge-poles to fit to data in the  $s$ -channel helicity amplitude was presented in Ref. [8]. A qualitative analysis of the process  $\gamma p \rightarrow \rho^\pm \Delta$  is made for a subprocess in the  $\pi$  photoproduction in Ref. [9]. However, all these are not complete to fully elucidate the production mechanism of such high-spin  $\Delta$ -baryon with the  $\rho$  from the standpoint of the effective Lagrangian formulation.

In previous works we investigated photoproduction of spin-1 vector meson on nucleon,  $\gamma N \rightarrow \rho^\pm N$  and  $\gamma N \rightarrow K^* \Lambda$  [10, 11], and that of spin-3/2  $\Delta$ -baryon  $\gamma p \rightarrow \pi^\pm \Delta$  [12] by using the Born amplitude where the  $t$ -channel meson exchanges were reggeized following the procedures of Ref. [13]. In all these reactions the energy-dependence of cross sections showed a common feature of the nondiffractive two-body scattering with a sharp

peaking behavior near threshold. From the standpoint of the Regge formalism, this can be understood by the relation,  $\sigma \sim s^{\alpha_J(0)-1}$ , which predicts the dominance of the  $\pi$  exchange over the  $\rho$  (and  $K$  over  $K^*$ ) to agree with the steep decrease observed in the total cross section beyond the resonance region. Indeed, our previous analyses on these photoproduction processes showed an agreement with such a production mechanism without either fit-parameters or *ad hoc* counter terms considered. On the other hand, the study of the former two processes served us to provide information on the EM multipole moments of the charged vector meson  $\rho(K^*)$ , and the case of the  $\pi\Delta$  process led us to consider a special gauge prescription (the minimal gauge) in order for a convergence of the cross section at high energy [14].

Hinted by these findings, we here investigate the  $\gamma p \rightarrow \rho^- \Delta^{++}$  process as a natural extension of our previous works, and our theoretical interest in the present issue is two-folded; the role of the EM multipole moments of  $\rho$ -meson and  $\Delta$ -baryon, and the convergence of the reaction cross section at high energy because both the propagators of the spin-1 and spin-3/2 particles have the term proportional to  $p^2/M^2$  which would diverge at high energy, unless one makes an approximation.

## The process with full propagations of $\Delta$ and $\rho$ : Model I

Since a particle of spin- $J$  has  $2J+1$  EM multipole moments, there are four EM multipole moments at the  $\gamma\Delta\Delta$  vertex in addition to the three multipole moments at the  $\gamma\rho\rho$  vertex in the charged process  $\gamma p \rightarrow \rho^- \Delta^{++}$ . This could cause further complication in establishing gauge invariance of the reaction process. As discussed in Ref. [10], the validity of the Ward identity for the  $\gamma\rho\rho$  coupling is crucial to render gauge invariance rather a simpler form. This is true for the  $\gamma\Delta\Delta$  vertex as well [12]. In this work, therefore, based on the Ward identities for

\* E-mail: bgyu@kau.ac.kr

† E-mail: kong@kau.ac.kr

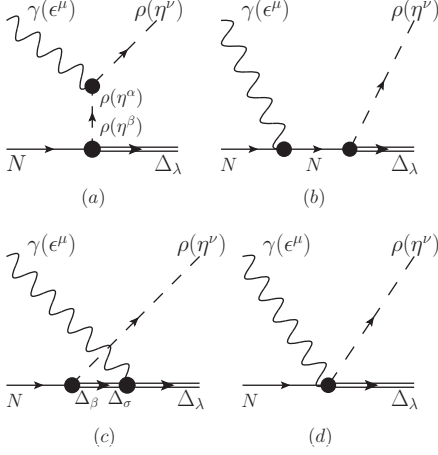


FIG. 1. Feynman diagrams for the gauge-invariant  $\rho$  exchange in  $\gamma(k) + N(p) \rightarrow \rho(q) + \Delta(p')$ .  $\pi$  and other meson exchanges proceed via the  $t$ -channel exchange (a).

the charge couplings in these vertices we first formulate a gauge invariant model for the  $\gamma p \rightarrow \rho^- \Delta^{++}$  process with the full propagators taken into account for both the  $\Delta$ -baryon and  $\rho$ -meson. This will make the model-description complete for the interaction between higher-spin particles with the EM multipole moments fully considered. We, then, proceed to the higher energy region to investigate the convergence of the reaction cross section.

For the photoproduction process

$$\gamma(k) + p(p) \rightarrow \rho^-(q) + \Delta^{++}(p'), \quad (1)$$

where the momenta of the initial photon, nucleon and the final  $\rho$  and  $\Delta$  are denoted by  $k$ ,  $p$ ,  $q$ , and  $p'$ , respectively, the current conservation following the charge conservation,  $e_p - e_{\rho^-} - e_{\Delta^{++}} = 0$ , requires the  $\Delta$ -pole in the  $u$ -channel in addition to the  $s$ -channel proton-pole and the contact term. Thus, we have the gauge-invariant  $\rho$  exchange in the  $t$ -channel which is given by

$$M_\rho = \bar{u}_\lambda(p') \eta_\nu^*(q) \times \left[ M_{t(\rho)}^{\lambda\nu\mu} + M_{s(p)}^{\lambda\nu\mu} + M_{u(\Delta)}^{\lambda\nu\mu} + M_c \right] \epsilon_\mu(k) u(p). \quad (2)$$

Here  $u_\lambda(p')$ ,  $u(p)$ ,  $\eta_\nu(q)$ , and  $\epsilon_\mu(k)$  are the spin-3/2  $\Delta$ -spinor of the Rarita-Schwinger field, Dirac spinor for nucleon, and the spin polarizations of  $\rho$  and photon. In Eq. (2) the respective particle exchanges and the contact term are given by

$$M_{s(p)}^{\lambda\nu\mu} = \Gamma_{\rho N \Delta}^{\lambda\nu}(q, p', p+k) \frac{\not{p} + \not{k} + M_N}{s - M_N^2} \Gamma_{\gamma N N}^\mu(k), \quad (3)$$

$$M_{t(\rho)}^{\lambda\nu\mu} = \Gamma_{\gamma \rho \rho}^{\nu\mu\alpha}(q, Q) \frac{-g_{\alpha\beta} + Q_\alpha Q_\beta / m_\rho^2}{t - m_\rho^2} \Gamma_{\rho N \Delta}^{\beta\lambda}(Q, p', p) \chi_A$$

$$M_{u(\Delta)}^{\lambda\nu\mu} = \Gamma_{\gamma \Delta \Delta}^{\lambda\mu\sigma}(k) \frac{\not{p}' - \not{k} + M_\Delta}{u - M_\Delta^2} \Pi_{\sigma\beta}^\Delta(p' - k) \times \Gamma_{\rho N \Delta}^{\beta\nu}(q, p' - k, p), \quad (5)$$

and

$$M_c = -\bar{u}^\lambda(p') \left\{ e_\rho \frac{f_{\rho N \Delta}}{m_\rho} (\epsilon_\lambda \not{q}^* - \eta_\lambda^* \not{q}) + \frac{g_{\rho N \Delta}}{m_\rho^2} [e_\Delta (q_\lambda \epsilon \cdot \eta^* - \eta_\lambda^* \epsilon \cdot q) + e_\rho (\epsilon_\lambda p' \cdot \eta^* - \eta_\lambda^* \epsilon \cdot p')] \right. \\ \left. + \frac{h_{\rho N \Delta}}{m_\rho^2} [e_N (q_\lambda \epsilon \cdot \eta^* - \eta_\lambda^* \epsilon \cdot q) + e_\rho (\epsilon_\lambda p \cdot \eta^* - \eta_\lambda^* \epsilon \cdot p)] \right\} \times \gamma_5 u(p) \quad (6)$$

with  $Q^\mu = (q - k)^\mu$ , the  $t$ -channel momentum transfer and the spin-3/2 projection which is given by

$$\Pi_{\mu\nu}^\Delta(p) = -g_{\mu\nu} + \frac{\gamma_\mu \gamma_\nu}{3} + \frac{\gamma_\mu p_\nu - \gamma_\nu p_\mu}{3M_\Delta} + \frac{2p_\mu p_\nu}{3M_\Delta^2}. \quad (7)$$

The electromagnetic coupling vertices  $\gamma N N$ ,  $\gamma \Delta \Delta$  [15] and  $\gamma \rho \rho$  [10] which fully account for their EM multipole moments are defined as follows,

$$\epsilon_\mu \Gamma_{\gamma N N}^\mu(k) = e_N \not{\epsilon} - \frac{e \kappa_N}{4M_N} [\not{\epsilon}, \not{k}], \quad (8)$$

$$\epsilon_\mu \Gamma_{\gamma \Delta \Delta}^{\lambda\mu\sigma}(p', k, p) = - \left\{ e_\Delta (g^{\lambda\sigma} \not{\epsilon} - \epsilon^\lambda \gamma^\sigma - \gamma^\lambda \epsilon^\sigma + \gamma^\lambda \not{\epsilon} \gamma^\sigma) - \frac{e}{4M_\Delta} \left( \kappa_\Delta g^{\lambda\sigma} + \chi_\Delta \frac{k^\lambda k^\sigma}{4M_\Delta^2} \right) [\not{\epsilon}, \not{k}] + \frac{e \lambda_\Delta}{4M_\Delta^2} \left[ k^\lambda k^\sigma \not{\epsilon} - \frac{1}{2} \not{k} (\epsilon^\lambda k^\sigma + \epsilon^\sigma k^\lambda) \right] \right\}, \quad (9)$$

$$\Gamma_{\gamma \rho \rho}^{\nu\mu\alpha}(q, Q) \epsilon_\mu = -e_\rho \left\{ \left[ (q + Q)^\mu g^{\nu\alpha} - Q^\nu g^{\mu\alpha} - q^\alpha g^{\mu\nu} \right] + \kappa_\rho (g^{\mu\alpha} k^\nu - g^{\mu\nu} k^\alpha) - \frac{(\lambda_\rho + \kappa_\rho)}{2m_\rho^2} \left[ (q + Q)^\mu k^\nu k^\alpha - \frac{1}{2} (q + Q) \cdot k (k^\nu g^{\mu\alpha} + k^\alpha g^{\mu\nu}) \right] \right\} \epsilon_\mu. \quad (10)$$

Here  $e_\Delta$ ,  $\kappa_\Delta$ ,  $\chi_\Delta$ , and  $\lambda_\Delta$  are the charge, anomalous magnetic moment, magnetic octupole, and electric quadrupole moments of the  $\Delta$ , respectively.  $e_\rho$ ,  $\kappa_\rho$  and  $\lambda_\rho$  are the charge, anomalous magnetic moment and electric quadrupole moment of  $\rho$ -meson.

Note that, in particular, the charge-coupling terms in Eqs. (8), (9), and (10) satisfy the Ward identities in their respective vertices [10, 12].

For the strong coupling vertex  $\rho N \Delta$  we utilized the following form from Ref. [7]

$$\Gamma_{\rho N \Delta}^{\lambda\nu}(q, p', p) = \left[ \frac{f_{\rho N \Delta}}{m_\rho} (q^\lambda \gamma^\nu - \not{q} g^{\lambda\nu}) + \frac{g_{\rho N \Delta}}{m_\rho^2} (q^\lambda p'^\nu - q \cdot p' g^{\lambda\nu}) + \frac{h_{\rho N \Delta}}{m_\rho^2} (q^\lambda p^\nu - q \cdot p g^{\lambda\nu}) \right] \gamma_5 \quad (11)$$

with the quark model prediction,  $f_{\rho^- p \Delta^{++}} = \frac{6\sqrt{2}}{5} f_{\rho^0 p p} = 8.57$ , which is from the relation  $\frac{f_{\rho^0 p p}}{m_\rho} = \frac{g_{\rho^0 p p}}{2M} (1 + \kappa_\rho)$

for the  $\rho$  exchange in the NN potential [16] and using  $g_{\rho^0 pp} = 2.6$  and  $\kappa_\rho = 3.7$  [10]. But, in consideration of the numerical results from a mesonic model [17] and other hadronic process [18] where the  $f_{\rho N\Delta}$  was determined to be smaller than the one discussed above we take the  $f_{\rho N\Delta}$  constant in the range from 4.7 to 8.6 in the calculation.

For a consistency with the previous work on  $\gamma N \rightarrow \rho^\pm N$  the EM multipole moments of  $\rho$ -meson,  $\kappa_\rho$  and  $\lambda_\rho$ , are taken the same as in Ref. [10]. The values for the EM multipole moments of the  $\Delta$ -baryon in Eq. (9) are taken from Ref. [15] for a complete set of these observables.

In the formal reggeization the gauge-invariant  $\rho$  exchange is now written as

$$\mathcal{M}_\rho = M_\rho \times (t - m_\rho^2) \mathcal{R}^\rho(s, t), \quad (12)$$

where

$$\mathcal{R}^\varphi(s, t) = \frac{\pi \alpha'_\varphi \times \text{phase}}{\Gamma(\alpha_\varphi(t) + 1 - J) \sin \pi \alpha_\varphi(t)} \left( \frac{s}{s_0} \right)^{\alpha_\varphi(t) - J} \quad (13)$$

is the Regge-pole written collectively for a meson  $\varphi$  of spin- $J$  with the phase and trajectory  $\alpha(t)_J$  [10]. The mass parameter is taken to be  $s_0 = 1 \text{ GeV}^2$ .

The gauge-invariant pion exchange in the  $t$ -channel is given by,

$$\begin{aligned} \mathcal{M}_\pi = & -i \frac{g_{\gamma\pi\rho}}{m_0} \frac{f_{\pi N\Delta}}{m_\pi} \varepsilon_{\mu\nu\alpha\beta} \epsilon^\mu \eta^{*\nu} k^\alpha Q^\beta \bar{u}_\lambda(p') Q^\lambda u(p) \\ & \times \mathcal{R}^\pi(s, t), \end{aligned} \quad (14)$$

where  $g_{\gamma\pi\rho} = \pm 0.224$  is estimated from the measured decay width and  $f_{\pi^- p \Delta^{++}}$  is chosen in the range from 1.7 to 2.16 [12] for a better agreement with existing data.

By using the coupling vertex  $a_2 N \Delta$  with the coupling constant  $\frac{f_{a_2 N \Delta}}{m_{a_2}} = -3 \frac{f_{\rho N \Delta}}{m_\rho}$  as in Ref. [12], and the vertex  $\gamma \rho a_2$  in Ref. [19] with the coupling constant  $0.044 \text{ GeV}^{-1}$  determined from the decay width [20] we estimate the contribution of the  $a_2$  exchange to find it to be of the  $10^{-2}$  order. Hence, it is neglected in this work.

Table I summarizes the physical constants for the Model I and Model II which are referred in advance for later use.

We now discuss the determination of the phases of  $\pi$  and  $\rho$  exchanges. Given the isospin relation for the different charge states of  $\rho N \Delta$  couplings

$$f_{\rho^- p \Delta^{++}} = f_{\rho^+ n \Delta^-} = \sqrt{3} f_{\rho^+ p \Delta^0} = \sqrt{3} f_{\rho^- n \Delta^+}, \quad (15)$$

and from the  $G$ -parity for photon-meson coupling which dictates the signs of  $\rho$  and  $b_1$  [10] to be changed in accord with their charges, we write the production amplitudes relevant to the present issue, i.e.,

$$M_{\gamma p \rightarrow \rho^- \Delta^{++}} = -M_\rho + M_{a_2} + M_\pi - M_{b_1}, \quad (16)$$

$$M_{\gamma n \rightarrow \rho^+ \Delta^-} = M_\rho + M_{a_2} + M_\pi + M_{b_1}. \quad (17)$$

In the absence of the  $a_2$  and  $b_1$  further, the situation is similar to the case of  $\gamma N \rightarrow \rho^\pm N$  [10]. In order to obtain a fair description of existing data up to  $E_\gamma \approx 10 \text{ GeV}$ , where the dominance of  $\pi$  exchange over the  $\rho$  is required

TABLE I. Physical constants in this work. Proton anomalous magnetic moment  $\kappa_p = 1.79$ .  $\rho$ -meson EM multipole moments  $\kappa_\rho = 1.01$  and  $\lambda_\rho = -0.41$  are fixed in both models. The effects from the multipole moments denoted as starred,  $\lambda_{\Delta^{++}}$  and  $\chi_{\Delta^{++}}$  are considered only in the limited energy region as in Fig. 2 (b). EM multipoles of  $\Delta$ -baryon are taken from Ref. [15].

	Model I	Model II
$\kappa_{\Delta^{++}}$	4.34	0
$\lambda_{\Delta^{++}}$	6.18*	0
$\chi_{\Delta^{++}}$	12.34*	0
$f_{\rho N \Delta}$	5.5	8.57
$g_{\rho N \Delta}$	0	0
$h_{\rho N \Delta}$	-2	0
$g_{\gamma\pi\rho^\pm}$	0.224	0.224
$f_{\pi N \Delta}$	1.7	2

for the steep decrease of the cross section we employ the phases given as follows,

$$\mathcal{M}(\rho^\mp) = \mp \rho \times \frac{1}{2}(-1 + e^{-i\pi\alpha_\rho(t)}) + \pi \times \left\{ \frac{1}{e^{-i\pi\alpha_\pi(t)}} \right\}. \quad (18)$$

In Fig. 2 we present the result of the Model I in the

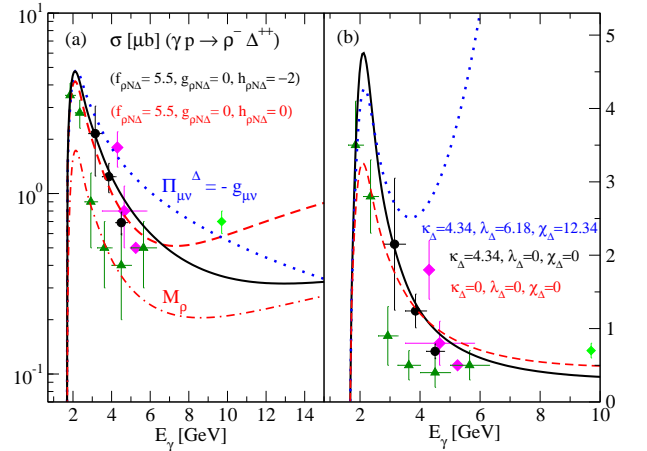


FIG. 2. Total cross section for  $\gamma p \rightarrow \rho^- \Delta^{++}$  from the Model I. (a): The cross section of the solid line shown in the log-scale becomes divergent above  $E_\gamma \simeq 10 \text{ GeV}$  due to the divergence of the  $u$ -channel  $\Delta$  over  $E_\gamma \simeq 7 \text{ GeV}$  in the gauge-invariant  $\rho$  exchange  $\mathcal{M}_\rho$  in Eq. (12) which is depicted by the red dash-dotted line. The nonvanishing  $h_{\rho N \Delta}$ -coupling plays the role to suppress the divergence of the cross section up to  $\approx 10 \text{ GeV}$ . The approximation of  $\Pi_{\mu\nu}^\Delta \approx -g_{\mu\nu}$  shows a large deviation with data. (b): Roles of the  $\Delta$ -baryon EM moments are shown in the total cross section. The cross section with EM moments fully accounted diverges over 4 GeV but yields the finite result below the energy region. Data are taken from Refs. [1, 3–5].

total cross section from the  $\rho + \pi$  exchanges with the trajectories

$$\alpha_\rho(t) = 0.9(t - m_\rho^2) + 1, \quad (19)$$

$$\alpha_\pi(t) = 0.7(t - m_\pi^2), \quad (20)$$

taken and physical constants from Table I. In both panels (a) and (b) the solid line represents the total cross section from the calculation with  $\kappa_\rho$ ,  $\kappa_{\Delta^{++}}$ ,  $\kappa_\rho$  and  $\lambda_\rho$  turned on in addition to their charges. Based on this, the cases of the vanishing constants  $g_{\rho N\Delta} = h_{\rho N\Delta} = 0$ , and the approximation of  $\Pi_{\mu\nu}^\Delta \approx -g_{\mu\nu}$  for the  $\Delta$ -propagation are tested, and they are found to be valid only in the limited range of energy as denoted by the red dashed, and blue dotted lines, respectively. In (b) the sensitivity of the cross section to the EM multipole moments of  $\Delta$  is examined and the role of  $\kappa_\Delta$  is found to be of significance as can be expected from the magnetic nature of the  $\Delta$ . Nevertheless, however, the prediction of the Model I with the EM multipole moments of  $\Delta$  fully accounted would fall down above  $E_\gamma \simeq 4$  GeV as shown by the dotted line. In both (a) and (b) the role of EM moments of  $\rho$  is much less significant than that of  $\Delta$ .

In the scheme where the spin-3/2 polarization tensor  $\Pi_{\mu\nu}^\Delta$  is fully considered for the  $\Delta$  propagation in the  $u$ -channel, we note that the cross section of the Model I as shown by the solid line is valid up to  $E_\gamma \simeq 10$  GeV with the energy-dependence finite. But it becomes divergent due to the  $u$ -channel divergence from the  $\Delta$ , though gauge-invariant.

In comparison to the  $\gamma p \rightarrow \pi^- \Delta^{++}$  process where the cross section already diverges about  $E_\gamma \simeq 1.7$  GeV [12], such a suppression of the divergence until 10 GeV in the present process may be due to the smaller coupling of  $\rho N\Delta$  with  $5.5/m_\rho$  than the  $\pi N\Delta$  coupling with  $1.7/m_\pi$  to the  $\Delta$ -pole in the  $u$ -channel.

In the next, let us consider the minimal gauge prescription for the conserved  $\rho$  exchange in order to render the cross section convergent far beyond the energy.

### The minimal gauge prescription: Model II

We apply the minimal gauge prescription for gauge invariance of the  $\rho$  exchange, where the proton and  $\Delta$  poles in the  $s$ - and  $u$ -channels are introduced in the minimal way, i.e., only the non-gauge-invariant remnant of the  $s$ - and  $u$ -channel electric Born terms are indispensable to compensate for the lack of the  $t$ -channel  $\rho$  exchange in the current conservation [14].

The gauge-invariant terms to be removed by redundancy is easily checked by replacing  $\epsilon$  with  $k$  and using the on-shell conditions  $\bar{u}_\lambda(p')\gamma^\lambda = 0$  in the EM vertices Eqs. (8) and (9). Then, similar to the  $\pi\Delta$  case as discussed in Ref. [12], the  $u$ -channel  $\Delta$ -pole as in Eq. (23) given below is obtained from such an antisymmetric form of the  $u$ -channel amplitude as in Eq. (12) of Ref. [12] due to the term  $-\epsilon^\lambda \gamma^\sigma$  in the  $\gamma\Delta\Delta$  vertex.

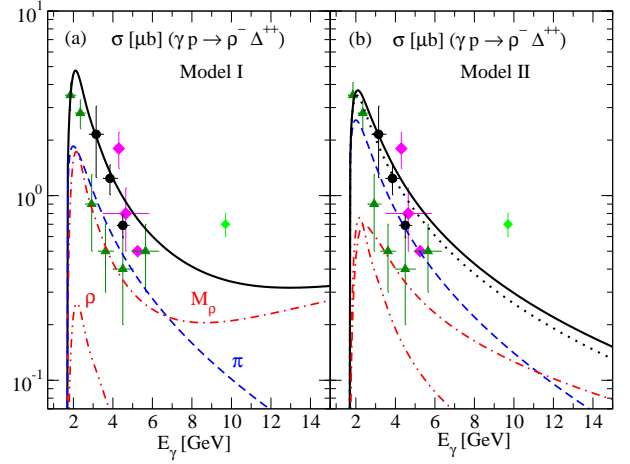


FIG. 3. Total cross section for  $\gamma p \rightarrow \rho^- \Delta^{++}$  from the Model I and II. (a): Contributions of the  $\pi$  and  $\rho$  exchanges in the  $t$ -channel and that of the  $M_\rho$  are given for comparison. (b): The cross section from the Model II shows a good convergence at high energy. The dotted line is the cross section without  $\rho$ -meson EM multipole moments  $\kappa_\rho$  and  $\lambda_\rho$ . Notations for curves are the same as in the panel (a). Data are taken from Refs. [1, 3–5].

The minimal gauge-invariant  $\rho$  exchange in Eq. (2) is now expressed as,

$$M_{s(p)}^{\lambda\nu\mu} = \frac{f_{\rho N\Delta}}{m_\rho} (q^\lambda \gamma^\nu - \not{q} g^{\lambda\nu}) \gamma_5 \frac{2p^\mu}{s - M_N^2} e_N, \quad (21)$$

$$M_{t(\rho)}^{\lambda\nu\mu} = \Gamma_{\gamma\rho\rho}^{\nu\mu\alpha}(q, k, Q) \frac{-g_{\alpha\beta} + Q_\alpha Q_\beta / m_\rho^2}{t - m_\rho^2} \times \frac{f_{\rho N\Delta}}{m_\rho} (Q^\lambda \gamma^\nu - \not{Q} g^{\lambda\nu}) \gamma_5, \quad (22)$$

$$M_{u(\Delta)}^{\lambda\nu\mu} = e_\Delta \frac{2p'^\mu}{u - M_\Delta^2} \frac{f_{\rho N\Delta}}{m_\rho} (q^\lambda \gamma^\nu - \not{q} g^{\lambda\nu}) \gamma_5, \quad (23)$$

with the contact term given in Eq. (6). A few remarks are in order: In the minimal gauge we neglect the terms of  $g_{\rho N\Delta}$  and  $h_{\rho N\Delta}$  couplings because of no need to suppress the divergence of the  $\Delta$ -pole. Strictly speaking, the  $\gamma\rho\rho$  vertex in Eq. (22) should also be simplified to have only the charge-coupling terms. Nevertheless we resume the original form to investigate the effects of the EM multipole moments.

Figure 3 shows the comparison of the cross sections between Model I and II with the contributions of meson exchanges therein. In Fig. 3 (b) we demonstrate a good convergence of the cross section at high energy by the dominating role of the  $\pi$  exchange over the  $\rho$  in the minimal gauge. In order to yield a better result from the Model II we use the coupling constants  $f_{\pi N\Delta} = 2$  and  $f_{\rho N\Delta} = 8.57$  which were adopted in the  $\gamma p \rightarrow \pi^- \Delta^{++}$  process [12]. We show the effect of the  $\rho$ -meson EM multipole moments  $\kappa_\rho$  and  $\lambda_\rho$  by the solid and dashed lines in (b).

Differential cross sections and density matrix elements

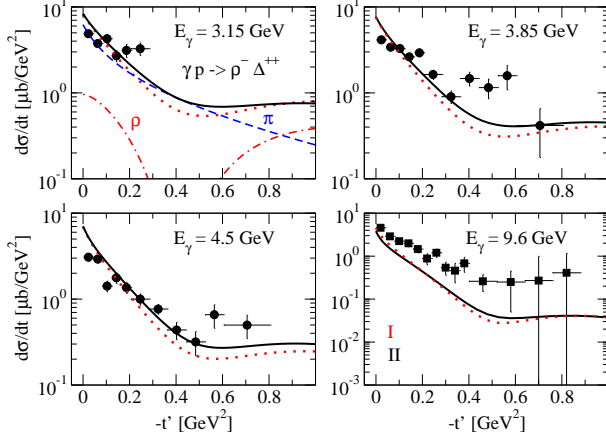


FIG. 4. Differential cross sections for  $\gamma p \rightarrow \rho^- \Delta^{++}$ . Contributions of  $\pi$  and  $\rho$  exchanges are shown in the dashed and dash-dotted lines at  $E_\gamma = 3.15$  GeV. The cross sections from the Model I (dotted) and II (solid line) are presented for comparison. Data are taken from Refs. [1, 2].

for the unpolarized process are given in Figs. 4 and 5, respectively. The contributions of  $\pi$  and  $\rho$  exchanges are shown at  $E_\gamma = 3.15$  GeV. The difference of the model predictions between I and II is presented for comparison. The angular dependence of the differential cross section is in fair agreement with the canonical phase taken for the  $\rho$  exchange which reproduces the dip at  $-t \approx 0.4$  GeV<sup>2</sup> by the nonsense-wrong-signature-zero at  $\alpha_\rho(t) = 0$ .

The density matrix elements presented in Fig. 5 are calculated in the Gottfried-Jackson (G.-J.) frame where the  $\rho \rightarrow \pi\pi$  decay with the  $\Delta$ -baryon in the final state is developed by following the conventions and definitions of Ref. [21]. Due to the canonical phase of the  $\rho$  exchange such an oscillatory behavior as in Fig. 5 could describe the  $t$ -dependence of the density matrix elements to some degree.

Finally, with an expectation of the magnetic nature of both the  $\Delta$  and  $\rho$  in the interaction with photon we make a prediction for the measurement of the magnetic moments of  $\Delta$  and  $\rho$  from the photon polarization asymmetry for future experiments. Figure 6 presents the photon polarization asymmetry  $\Sigma$  with and without  $\kappa_\Delta$  with respect to the angle (a) and energy (b), respectively. Likewise, the cases of the  $\rho$  with and without the EM multipole moments are given in the row (c) and (d).

To summarize, we have investigated the photoproduction  $\gamma p \rightarrow \rho^- \Delta^{++}$  process with a particular interest in the role of the  $\rho$  and  $\Delta$ -baryon EM multipole moments as well as the convergence of the cross section at high energy. By constructing two versions in order to treat the divergence of the  $\Delta$ -propagation in the  $u$ -channel, the so-called Model I and II, we examined the energy dependence of the cross section up to  $E_\gamma = 10$  GeV and 16 GeV, respectively. The important findings in the present work are as follows: We observed a strong peak in the

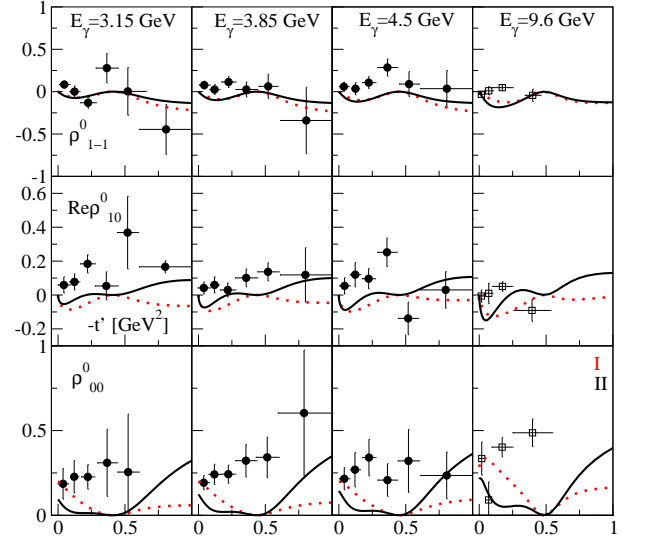


FIG. 5. Density matrix elements  $\rho^0_{\lambda\lambda'}$  at the G.-J. frame for the  $\rho \rightarrow \pi\pi$  decay in the unpolarized process  $\gamma p \rightarrow \rho^- \Delta^{++}$ . Notations for the curves are the same as in Fig. 4. Data are taken from Refs. [1, 2].

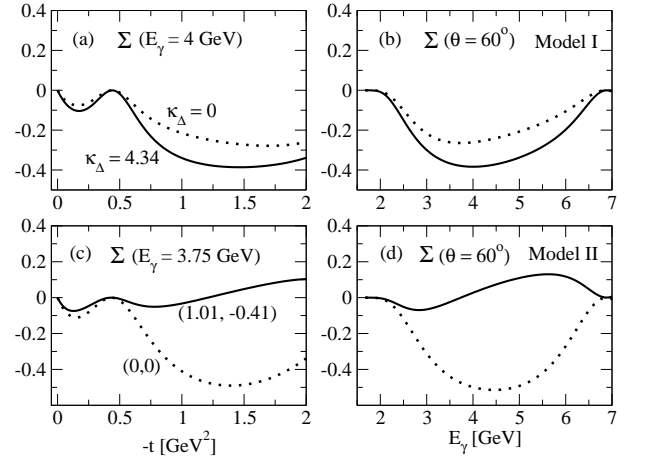


FIG. 6. Sensitivity of photon polarization asymmetry  $\Sigma$  to magnetic moments of  $\Delta$  in the Model I and  $\rho$  in the Model II.  $\Sigma$  with and without  $\kappa_\Delta$  are presented in (a) and (b) with respect to  $-t$  and  $E_\gamma$ . The row (c) and (d) are the case of the  $\rho$  with and without  $\kappa_\rho$  and  $\lambda_\rho$ .

forward-scattering region due to the nondiffractive  $\pi + \rho$  exchanges in the  $t$ -channel. The steep decrease of the total cross section is well reproduced by the dominance of the  $\pi$  exchange over the  $\rho$ , and the canonical phase thus assigned to the  $\rho$  exchange describes the data with the dip-pattern in the differential cross section as well as the oscillatory behavior of the density matrix elements.

Therefore, both the Model I and II can be appreciated to yield the results valid up to  $E_\gamma \simeq 10$  GeV. In particular, the former model has the advantage of investigating

the EM multipole moments of  $\Delta$ -baryon in the low energy region below  $E_\gamma \simeq 3$  GeV, while the latter could provide a reliable base to explore the higher energy region beyond 10 GeV without divergence.

The present theoretical results would be useful to guide and estimate for the high-energy photon-beam experiment, such as the future experiments in the LEPS2 at

SPRING-8 and CLAS12 at the Jefferson lab.

## ACKNOWLEDGMENT

This work was supported by the grant NRF-2013R1A1A2010504, and by the grant NRF-2016K1A3A7A09005580 from National Research Foundation (NRF) of Korea.

- 
- [1] D. P. Barber *et al.*, Z. Phys. C **2**, 1 (1979).
  - [2] J. Abramson *et al.*, Phys. Rev. Lett. **36**, 1432 (1976)
  - [3] W. Struczinski *et al.*, Nucl. Phys. B **108**, 45 (1976).
  - [4] C. A. Nelson *et al.*, Phys. Rev. D **17**, 647 (1978).
  - [5] Y. Eisenberg, B. Haber, E. E. Ronat, A. Shapira, and G. Yekutieli, Phys. Rev. Lett. **25**, 764 (1970).
  - [6] J. Ballam *et al.*, Phys. Rev. Lett. **26**, 995 (1971).
  - [7] R. B. Clark, Phys. Rev. D **1**, 2152 (1970).
  - [8] M. Clark and A. Donnachie, Nuclear Materials B **125**, 493 (1977).
  - [9] J. M. Laget, Phys. Lett. B **695**, 199 (2011).
  - [10] B.-G. Yu and K.-J. Kong, arXiv:1604.03691 [nucl-th].
  - [11] B.-G. Yu, Y. Oh, and K.-J. Kong, arXiv:1608.00455 [hep-ph].
  - [12] B.-G. Yu and K.-J. Kong, arXiv:1611.09629 [hep-ph].
  - [13] M. Guidal, J. M. Laget, and M. Vanderhaeghen, Nucl. Phys. A **627**, 645 (1997).
  - [14] J. A. Campbell, R. B. Clark and D. Horn, Phys. Rev. D **2**, 217 (1970).
  - [15] K. Azizi, Eur. Phys. J. C **61**, 311 (2009) arXiv:0811.2670 [hep-ph].
  - [16] G.E. Brown and W. Weise, Phys. Rep. C **22**, 279 (1975).
  - [17] Q. Haider and L. C. Liu, Phys. Lett. B **335**, 253 (1994)
  - [18] H. Kamano and M. Arima, Phys. Rev. C **69**, 025206 (2004).
  - [19] B.-G. Yu, H. Kim, and K.-J. Kong, arXiv:1611.01345 [hep-ph].
  - [20] S. Ishida, K. Yamada, and M. Oda, Phys. Rev. D **40**, 1497 (1989).
  - [21] K. Schilling, P. Seyboth and G. E. Wolf, Nucl. Phys. B **15**, 397 (1970) [Erratum-ibid. B **18**, 332 (1970)].